Singh *et al. Biochar* (2024) 6:17
https://doi.org/10.1007/s42773-024-00306-5

Biochar

ORIGINAL RESEARCH

Open Access

Effect of biochar on soil microbial community, dissipation and uptake of chlorpyrifos and atrazine

Raghvendra Pratap Singh[1], Ranu Yadav[1,3], Versha Pandey[1,3], Anupama Singh[1,3], Mayank Singh[1,3], Karuna Shanker[2,3] and Puja Khare[1,2*]

Abstract

For the application of biochar in restoring pesticide-contaminated soils and minimizing the risk associated with their uptake in plants, it is crucial to understand the biochar impact on soil biological activities and dissipation and accumulation of pesticides in plant and soil systems. In this study, the effect of *Mentha*-distilled waste-derived biochar was investigated on chlorpyrifos and atrazine contaminated sandy loam soil. The four application rates of atrazine (2, 4, 6, and 8 mg kg^{-1}) and chlorpyrifos (2, 4, 6, and 12 mg kg^{-1}) and a single application rate of biochar (4%) were used in this study. The degradation of pesticides, the diversity of the bacterial community, and enzymatic activities (alkaline phosphatase, dehydrogenase, arylsulfatase, phenol oxidase, urease activity and *N*-acetyl glucosaminidase) were examined in soil. The uptake of two pesticides and their effect on growth and stress parameters were also investigated in plants (*A. paniculata*). The dissipation of chlorpyrifos and atrazine followed simple first-order kinetics with a half-life of 6.6–74.6 and 21–145 days, respectively. The presence of deisopropyl atrazine desethyl atrazine (metabolites of atrazine) and 3,5,6-trichloro-2-pyridinol (a metabolite of chlorpyrifos) was observed in soil and plant tissues. Biochar application significantly ($p=0.001$) enhanced the degradation rate of chlorpyrifos and atrazine leading to the lower half-life of chlorpyrifos and atrazine in soil. A significant reduction ($p=0.001$) in the uptake of chlorpyrifos and atrazine and alteration in their binding affinity and uptake rate in plant tissues was observed in biochar treatments. The incorporation of biochar improved chlorpyrifos/atrazine degrader and plant growth-promoting bacterial genera such as *Balneimonas*, *Kaistobacter*, *Rubrobacter*, *Ammoniphilus*, and *Bacillus*. The upregulation of functional genes associated with nucleotide, energy, carbohydrate, amino acid metabolism, xenobiotic biodegradation, and metabolism: atrazine degradation was observed in biochar treatments. The biochar amendments significantly ($p=0.001$) reduced the plant's uptake velocity (Vmax) and affinity (Km) of chlorpyrifos and atrazine. These results delineated that Mentha-distilled waste-derived biochar can potentially remediate chlorpyrifos and atrazine contaminated soils and ensure the safety of plants for consumption.

Handling editor: Bin Gao

*Correspondence:
Puja Khare
pujakhare@cimap.res.in; kharepuja@rediffmail.com
Full list of author information is available at the end of the article

Highlights

- Biochar amendments reduced the half-life of chlorpyrifos and atrazine in soil.
- Biochar altered the binding affinity and uptake rate of chlorpyrifos and atrazine in plant tissues.
- Biochar up-regulated gene assigned to xenobiotic, energy, and carbohydrate metabolism in soil.
- Biochar enhanced *Pseudomonas* and *Bacillus* species in soil.

Keywords Chlorpyrifos, Atrazine, Dissipation, Uptake kinetics, Biochar

Graphical Abstract

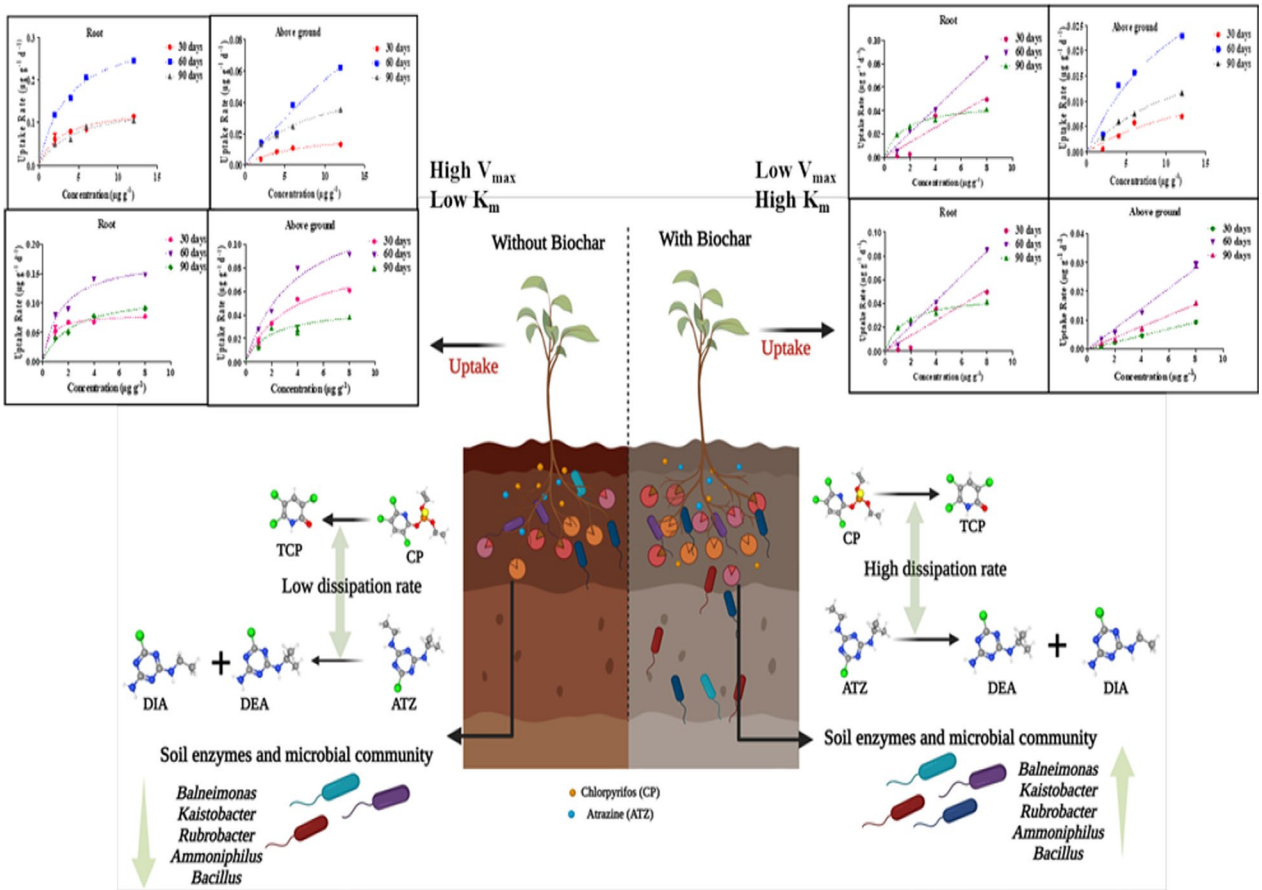

1 Introduction

The excessive use of pesticides has harmful effects on the ecosystem as well as on human health. Chlorpyrifos (*o*,*o*-diethyl *o*-(3,5,6-trichloro-2-pyridinyl)-phosphorothioate) is widely used pesticide in agriculture due to its lower cost and minimum effect on the germination of seed (Anbarasan et al. 2022; Mahajan et al. 2023). From 2014–2018, chlorpyrifos (CP) was annually used (approximately 25,500 tons) in a wide range of crops (Foong et al. 2020). The expansion of CP uses in agriculture was estimated to be up to 5000 tons in India and over 28,600 tons worldwide (Mishra et al. 2021; Paidi et al. 2021). Likewise, atrazine has been used to control grassy and broadleaf weeds for the last four decades (Shekhawat et al. 2020). The annual consumption of atrazine (ATZ) is 7×10^4–9×10^4 tons worldwide and 340 tons annually in India (Singh et al. 2018). The half-lives of CP and ATZ varied from 60–120 days and 37–326 days, respectively, depending upon the biological and chemical status of the soil (Farhan et al. 2021). The CP is hydrophobic,

while ATZ is a weak base (pKa = 1.67) and can ionized at a higher pH than its pKa. Their octanol–water partition coefficients ranged between 2.61–4.66 and were highly affixed to the organic carbon (Garrido et al. 2019; Torres and Coelho 2023). The persistent metabolite of CP, i.e., 3,5,6-trichloro-2-pyridinol (TCP), has a higher toxicological effect and half-life (65–360 days) in soil than its parent molecule (Bose et al. 2021). The ATZ on degradation produced deisopropyl atrazine (DIA), desethyl atrazine (DEA), and hydroxyl atrazine (HA) in soil, which has similar toxicological effects on soil microbiota (Kumar and Singh 2016). The presence of CP and ATZ and their metabolites higher than the permitted limit was observed in groundwater, agricultural soil, vegetables, and fruit samples (Hasanuzzaman et al. 2018; Bose et al. 2021). Their occurrence in groundwater, plants, and soil is hazardous for flora and fauna (Bhende et al. 2022). In soil, both CP and ATZ have an inhibitory effect on enzymatic activities and altered the soil metabolic process and nutrient mineralization, hence impairing the plant growth (Fan et al. 2020; Yadav and Khare 2023).

Over the last two decades, biochar produced by incomplete combustion of biomass has been considered a promising option for immobilizing the pollutants in the soil due to its porous structure and surface properties (Zhou et al. 2021). The application of biochar displayed a beneficial effect on its fertility and soil biological activities and improved the growth of plants (Nigam et al. 2019; Jain et al. 2020; Singh et al. 2022b; Yadav et al. 2023). Song et al. (2023) in his review demonstrated that biochar has high adsorption potential and can accelerate the pesticide degradation of soil and mitigate its uptake in the plantings. Therefore, biochar application in pesticide-contaminated soil can be a good option for minimizing the risk associated with the consumption of contaminated agricultural produce (Li and Fantke 2023; Song et al. 2023).

The adsorption of CP and ATZ by biochar was well documented in several studies (Jacob et al. 2020; Diao et al. 2021; Singh et al. 2022a). Most of the studies on biochar were focused on its adsorption behavior and removal of pesticides from the water bodies (Cao et al. 2023; Eissa et al. 2023). The effects of various biochar amendments on CP/ATZ contaminated different types of soils were examined for remediation purposes (Singh et al. 2022b; Dong et al. 2023; Liu et al. 2023b; Qie et al. 2023; Zhang et al. 2023). The fate of CP/ ATZ in soil and the alteration in biological activities by biochar were also reported by different authors (Cheng et al. 2023; Yadav et al. 2023). The ameliorative effect of biochar on plants under chlorpyrifos stress was also observed (Huang et al. 2022; Shen et al. 2022). However, all these studies described the impact of biochar on pesticide contamination in individual systems; however, a comprehensive investigation of the effects of biochar on plant-soil-microbial communities with pesticides, particularly CP and ATZ, has not been well-studied. We hypothesized that adding biochar to CP/ATZ-contaminated soil can affect the dissipation of contaminants and their uptake by plants. We believe changes in the soil microbial community and enzymatic activities are linked to uptake and degradation processes. To validate the above hypothesis, the present study examined the effect of biochar on CP and ATZ dissipation in soil and uptake in the plant, plant growth, enzyme activities, and microbial community of soil. The author's best knowledge of the data on the linkage between the change in microbial community and dissipation in soil and uptake kinetics of CP and ATZ in plants is not reported. In this study, an experiment was conducted on Andrographis paniculata (Burm. f.) Nees, an annual herbaceous medicinal plant. The plant contained andrographolide, flavonoids, and polyphenols (Chao and Lin 2010). Andrographolide is a significant compound because of its pharmacological properties (Kumar et al. 2021). The dry leaves of plants are used as a traditional medicine and reported its therapeutic potential for mild to moderate COVID-19 (Gaur et al. 2021, 2023).

2 Materials and methods

2.1 Materials

For the experiment, the soil was taken from fallow land of an experimental form of CSIR-Central Institute of Medicinal and Aromatic Plants (CSIR-CIMAP), Lucknow, India (26° 48′ 0″ N, 80° 54′ 0″ E) at a depth of 0–15 cm. The distilled waste of *Mentha arvensis* was used to produce biochar according to previously reported conditions (Nigam et al. 2019). Fine powdered and sieved (2-mm particle size) soil and biochar were used for the experiment. The properties of biochar and soil are given in the Additional file 1: Ia. The high purity grade (99%) and the commercial-grade CP and ATZ were purchased from Sigma-Aldrich (USA) and the local market (Rasayanzine Weedicides in Hemkunt Tower Nehru Place, New Delhi), respectively.

2.2 Experimental design and sampling

For this study, a pot trial was performed in a random block design. The four-application rates of atrazine (2, 4, 6, and 8 mg kg^{-1}) and CP (2, 4, 6, and 12 mg kg^{-1}) were taken in the soil to evaluate their dissipation in soil and uptake kinetics in plants. The typical application rates of CP and ATZ in agricultural soils were reported as 3–6 mg kg^{-1}. Hence, these rates and lower and higher application rates were chosen for the study (Sánchez et al. 2017). Simultaneously, control was prepared as unspiked soil with and without biochar (n = 3 each). The

application rate of biochar (4%) was chosen according to a previous study showing the ameliorative effect of biochar at this dose on different types of pesticide-contaminated soil (Singh et al. 2022b). The experiment was performed in a 5 kg homogenous mixture of soil with and without biochar in triplicates. Before the investigation, the homogeneity of pesticide concentration in each treatment was checked, and no significant difference was observed among the soil samples. The nomenclature of the treatments in the manuscript was the control as Con, and CP treatments named C1, C2, C3, and C4 for the application rate of 2, 4, 6, and 12 mg kg^{-1}, respectively and ATZ treatments named A1, A2, A3, and A4 for application rates 2, 4, 6, and 8 mg kg^{-1}, respectively. The biochar treatments were named by adding B in the respective soil treatments, i.e., biochar treated in C1 is named C1B.

All the prepared pots were left for 7 days and water holding capacity (40%) was maintained during the period. Then 2 months old plantlets of *A. paniculata* were transferred in pots (three plantlets per plot) and irrigated regularly. For the dissipation and uptake kinetic study, rhizospheric soil and plant samples were collected at 30, 60, and 90 days. Fresh weights of plants were taken after cleaning with deionized water. The biomass of the sample collected at 90 days was reported here. The protein, chlorophyll, and stress enzymes were analyzed in fresh leaf samples collected at 90 days. The shade-dried and finely powdered plant tissues (root, stem, and leaf) were used for pesticide analysis.

The soil samples were taken from a rhizospheric portion of the plant and divided into two parts, i.e., one used for the analysis of CP/ATZ, pH, microbial biomass carbon, and enzymatic of soil and stored at 4 °C. However, another part was used for bacterial metagenome and stored at −20 °C. The samples of control, A4, A4B, C4, and C4B treatments collected at 30 and 90 days were used for the pH, microbial biomass carbon, enzymes, and molecular analyses.

2.3 Analysis of CP and ATZ

The QuEChERS method was used to extract and clean CP and ATZ from soil and plant samples. A 1.0 g sample was taken in acetonitrile (4 mL) and then centrifuged (8000g). The supernatant was extracted using a mixture of NaCl (50 mg) and anhydrous $MgSO_4$ (150 mg). For the clean-up process, a combination of anhydrous $MgSO_4$ (150 mg), primary-secondary amine (25 mg), and graphitized carbon black (25 mg) was used. After clean-up, the supernatant was vortexed and centrifuged for 5 min at a speed of 8000×*g*. Then the solution was concentrated by the rotatory evaporator and re-suspended in acetonitrile to the same volume (Mac Loughlin et al. 2022).

High-performance liquid chromatography (Model: SPD-M20A make: Shimadzu, Japan) was used for the analysis of CP and TCP. The stationary and mobile phases were C18 reversed-phase column (2.1 mm × 50 mm and 1.8 µm particle size) and acetonitrile/water (90:10), respectively. The flow rate of mobile phase and the oven temperature were 1 mL min^{-1} and 30 °C, respectively. The photodiode array detector (PDA) at wavelength 290 nm was used for the identification of pesticide (Yadav et al. 2023). The quality control parameters of CP and TCP in soil were recoveries: 97.59% and 93.7%; LOD; 0.005 mg kg^{-1} and 0.0046 mg kg^{-1}, LOQ; 0.015 mg kg^{-1} and 0.0139 mg kg^{-1}, respectively. The quality control parameters of CP and TCP in plant tissues were 95.6% and 91.6%, LOD; 0.0031 mg kg^{-1} and 0.0029 mg kg^{-1}, LOQ; 0.0095 mg kg^{-1} and 0.0088 mg kg^{-1} respectively.

The ATZ and its metabolites were analysed by gas chromatography (Agilent 7890B) equipped with an electron capture detector and column DB-5 (30 m × 250 µm × 0.25 µm) using nitrogen as carrier gas. The oven temperature conditions were 150 °C (hold for 5 min), ramp 1 rate of 8 °C min^{-1}, 280 °C (hold for 10 min), ramp 2 rate of 8 °C min^{-1}, and 300 °C (hold for 10 min), the total run time was 43 min. The injection volume and the flow of carrier gas were 2 µL and 30 mL min^{-1} respectively. The temperatures of the inlet and detector were 250 °C and 310 °C, respectively. The quality control parameters of ATZ, DIA, and DEA in soil were recoveries 94.65–95.27%, LOD: 0.006–0.009 mg kg^{-1}, and LOQ: 0.023–0.03 mg kg^{-1}. However, their quality control parameters in the plant were recoveries 91–95%, LOD: 0.007–0.009 mg kg^{-1}, and LOQ: 0.021 -0.030 mg kg^{-1}.

2.4 Plant growth and stress parameters

Total chlorophyll content in fresh leaves was determined by the method of Arnon and Whatley (1949). For soluble protein content, the fresh leaves were ground in a 1 mL phosphate buffer (pH 7.0). The bovine serum albumin (BSA) and Bradford reagent were added and the absorbance of the samples was taken at 595 nm in a spectrophotometer (Bradford 1976). For stress enzymes, the leaf tissue was homogenized in 1.5 mL of phosphate buffer (pH 7.5 containing) and then centrifuged at 4 °C for 20 min at 15,000×*g*. Superoxide dismutase activities were determined using photochemical reduction of NBT (Nitrobluetetrazolium), and absorbance was monitored at 560 nm (Beauchamp and Fridovich 1971). Catalase activity in leaf tissues was analyzed according to the method described by Luck (1974) and a decrease in absorbance due to dissociation of H_2O_2 was recorded spectrophotometrically at 240 nm. The proline contents

in fresh leaves were determined according to the method of (Bates et al. 1973).

The secondary metabolite contents in *A. paniculata* were measured in dried and found ground leaves. For this, the leaf extract was prepared in methanol and concentrated in a rotary evaporator. The 1 mL of methanol was added to the dried extract which was filtered through a syringe filter (PVDF 0.22 µm) and stored in vials at 4 °C. The analysis was performed using high-performance liquid chromatography (model SPD-M20A, Shimadzu Japan) with reverse-phase C18 column (flow rate: 1 mL/min; injection volume: 10 µL) and PDA detector at 223 nm. The phosphate buffer (potassium dihydrogen orthophosphate and orthophosphoric acid) and acetonitrile were used as mobile phase (Das et al. 2021). Bioconcentration factor (BCF) of CP/ATZ of *A. paniculata* was calculated by dividing the CP/ATZ content in the plant by the content in the soil. The translocation factor (TF) of CP and ATZ of *A. paniculata* was the ratio of CP and ATZ content in above-ground plant tissues and the soil.

2.5 Soil analysis

The pH analysis of the soil in different treatments was done using Mettler Seven Go DuoTM pH/Conductivity meter SG23. Soil microbial biomass carbon (SMBC) was analyzed using the fumigation extraction method (Yuan et al. 2021). Alkaline phosphatase, dehydrogenase, arylsulfatase, phenol oxidase, urease activity and *N*-acetyl glucosaminidase were determined in soil by previously reported methods (Casida Jr et al. 1964; Tabatabai and Bremner 1972; Eivazi and Tabatabai 1977, 1988; Bach et al. 2013; Acosta-Martinez et al. 2018). The activities of alkaline phosphatase, arylsulfatase, and *N*-acetyl glucosaminidase were expressed in µg PNP g^{-1} soil. The activities of dehydrogenase and phenol oxidase enzymes were expressed as µg TPF g^{-1} soil and µmol L DOPA g^{-1} soil, respectively. The urease activity was expressed as µg NH_4^+-Urease g^{-1} soil.

2.6 Metagenome analysis

The metagenome analysis was used only for bacterial genera in three biological replicates of each sample studied. A commercially available soil kit (Nucleospin Soil) was used for soil DNA extraction with some modifications. DNA quality and yield were estimated by Nanodrop spectrophotometer, Qubit dS DNA HS assay kit, and gel electrophoresis. The 16S rRNA gene was amplified using forward (5′ TCGTCGGCAGCGTCAGATGTGTATAAGAGACAGCCTACGGGNGGCWGCAG 3′) and reverse (5′ GTCTCGTGGGCTCGGAGATGTGTATAAGAGACAGGACTACHVGGGTATCTAATCC 3′) primers, which cover the V3-V4 region of the 16S rRNA gene and produce an amplicon of ~460 bp. Details of PCR amplifications have been reported previously (Singh et al. 2021). The sequences obtained were combined with overlapping, the primers were trimmed, and the sequences were replicated. The chimeric sequences were identified and removed using QIIME. The bases at the 5′ and 3′ regions with a Q score lower than 20 were also removed. Each sequence obtained was grouped into OTUs according to their similarity. OTU clustering was done by Qiime and Vsearch (1.9.6). An index such as Shannon was analyzed in QIIME. The generated OTU table after metagenome analysis was imported into the PICRUSt (version 1.1.0) and was used to predict changes in the functional protein-coding genes of the various microbial communities (Zhou et al. 2022; Yadav and Khare 2023).

2.7 Kinetic model parameters

The single first order (SFO) kinetics model (Eq. 1) was applied for CP and ATZ dissipation in soil and their uptake in plants (Singh et al. 2022b).

$$Y = Y0 + (P - Y0) * 1(-\exp(-k * T) \quad (1)$$

where Y = CP/ATZ content in soil/plant tissues at a given time; Y0 = Initial content of CP/ATZ in soil/plant tissues at a given time; k = rate constant; P = Plateau, T = time in days.

The root mean square error (RMSE) was used for method validation. The Michaelis–Menten equation was used for CP/ATZ uptake kinetics (Yadav and Khare 2023).

2.8 Statistical analysis

The descriptive statistical tests, one-way analysis of variance (Tukey's post hoc test), and Pearson Correlation were applied to the data set using SPSS software (version 25.0, IBM SPSS-21). GraphPad Prism version 5.00 was employed to assess kinetic modeling. The multivariate analyses such as correspondence (CA), principal component (PCA), and clustered heatmap were performed by using *FactoMineR, factoextra, ade4, magrittr, and pheatmap* packages in R (Version 4.2.0) software. Correspondence analysis is a statistical method that simplifies the complex dataset in a straightforward and often two-dimensional space. PCA is an orthogonal mathematical transformation and generates principal components (PC) that account for the majority of the variance in the data. Both techniques can visualize the relationship not only among row or column variables but also between row and column variables in a very bulky data set (Andrade et al. 2020). The data were normalized through logarithmic transformation for multivariate analyses.

3 Results

3.1 Degradation of chlorpyrifos and atrazine in soil

In unamended soil, the decrease in CP and ATZ concentrations in soil within 90 days were 28–60% and 46–56%, respectively (Additional file 1: II). However, in biochar treatments, decreases in CP and ATZ concentration in soil were 44–76% and 55–77%, respectively. Among the treatments, a rapid decline in CP content in soil was observed at a lower application rate (C1 and C1B). In comparison, speedy degradation of ATZ in soil was observed at its higher application rate.

The degradation kinetics of CP and ATZ in soil followed simple first-order kinetic with a high regression coefficient ($R^2 = 0.996–0.999$) and low root mean square error (0.004 to 0.113) (Fig. 1 and Additional file 1: III). In unamended soil, the half-life of CP and ATZ were 8.3–74.6 days and 21–145 days, respectively. The dissipation constant of CP and ATZ were 0.009–0.083 d^{-1} and 0.005 to 0.033 d^{-1}, respectively. However, in biochar treatments, the half-life of CP and ATZ was 6.6–41.1 days and 40–76 days, respectively. The dissipation constants of CP and ATZ were 0.017–0.104 d^{-1} and 0.009–0.017 d^{-1}, respectively, in biochar treatments. First-order kinetics for degradation showed higher plateau values for both pesticides in unamended soil than in biochar-amended soil. The plateau values for CP degradation ranged from 0.416 to 2.33 in unamended treatments and −0.333 to 1.853 in biochar amendments. The values of the plateau were enhanced with the application rate of CP. Atrazine plateau values were −6.874 to 1.632 in unamended soil and −4.286 to 0.236 in biochar treatments. No pattern was observed in plateau values with the application rate of atrazine.

3.2 Uptake and kinetics of chlorpyrifos and atrazine in plant

In plants, CP and ATZ more accumulated in root tissues than in above-ground tissues. In unamended soil, the concentrations of CP and ATZ in root tissues were 2.2–9.46 μg g^{-1} and 0.87–8.16 μg g^{-1}, respectively. However, above-ground tissues had 0.13–3.17 μg g^{-1} CP content and 0.61–3.44 μg g^{-1} ATZ content. In biochar treatments, CP concentrations were 0.23–4.25 μg g^{-1} in root tissues and 0.02–1.04 μg g^{-1} in above-ground plant tissues. The ATZ content was 0.045–3.70 μg g^{-1} in root and 0.02–1.435 μg g^{-1} in above-ground plant tissues of biochar treatments (Additional file 1: II). There was a significant increase in the CP and ATZ concentrations in plant tissues with time.

In unamended soil, the bio-concentration factor (BCF) and translocation factor (TF) of CP ranged from 0.78–2.17 and 0.27–0.55, respectively. The BCF and TF of ATZ in plants were from 0.02–3.54 and 0.32–0.58, respectively. In biochar treatments, values of BCF and TF of CP were 0.35–1.23 and 0.08–0.19, respectively. However, in biochar treatments, the BCF and TF of ATZ were 0.46–1.75 and 0.04–0.66, respectively (Additional file 1: II).

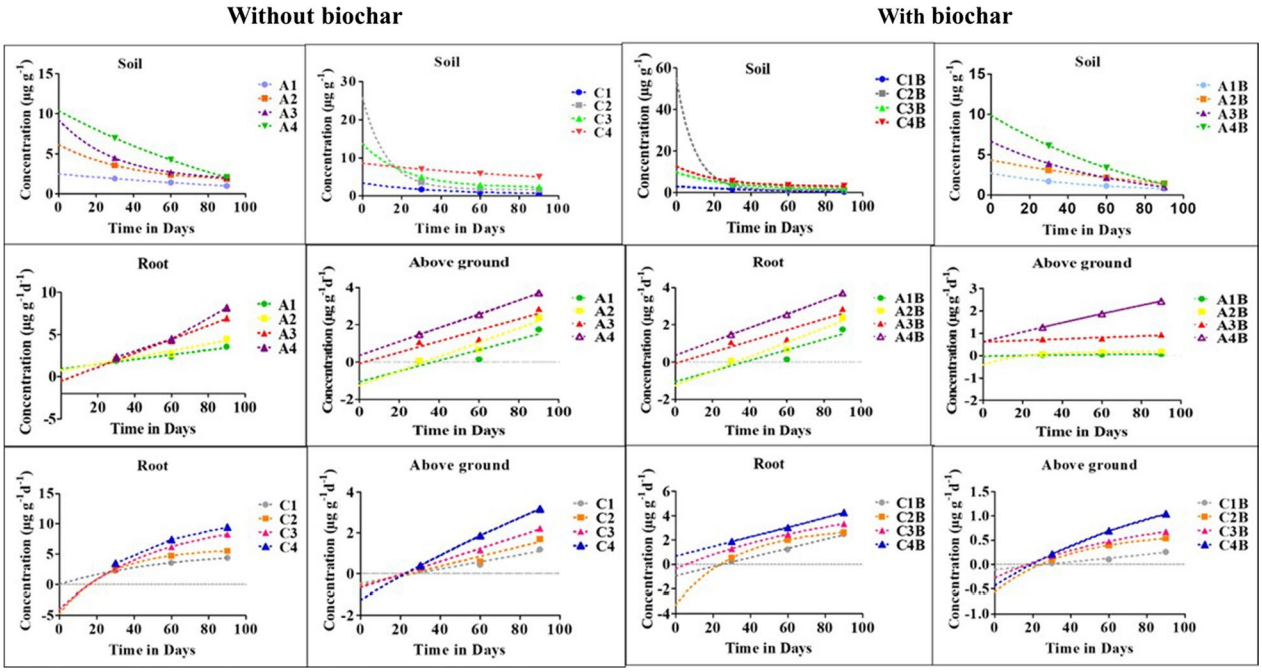

Fig. 1 Dissipation and uptake kinetics of chlorpyrifos and atrazine with and without biochar treatments

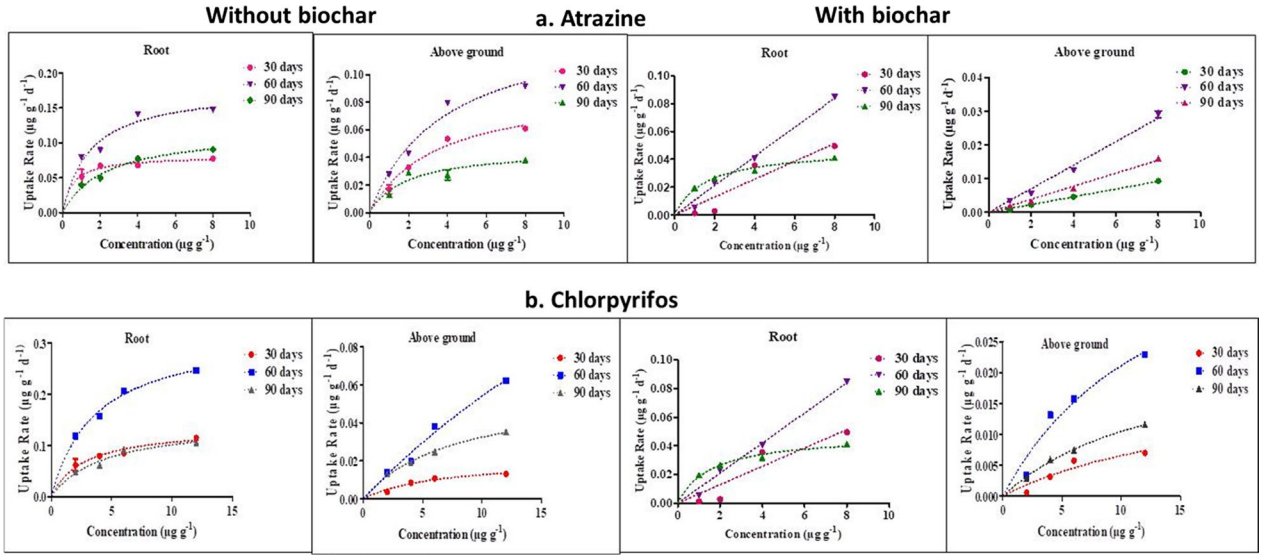

Fig. 2 Michaelis–Menten kinetics for chlorpyrifos and atrazine uptake in *A. Panniculata*

The uptake kinetics demonstrated that first-order kinetics was fitted in all treatments in root samples and C4 in above-ground tissues of unamended soil (Fig. 1 and Additional file 1: IV). Among biochar treatments, CP uptake followed first-order kinetics in C2B and C3B treatments of root and C2B, C3B, and C4B of above-ground tissues. ATZ uptake followed first-order kinetics only in above-ground tissues of A3, A4, A3B, and A4B treatments.

The Michaelis–Menten kinetics was also applied for CP and ATZ uptake in *A. paniculata* (Fig. 2 and Additional file 1: V). In unamended soil, the Vmax and Km values of CP in root tissues were 0.2373–0.2559 µg g^{-1} d^{-1} (with maximum value at 60 days) and 6.285–3.394 µg, respectively. However, in biochar treatments, Vmax and Km values in root tissues for CP were 0.07693–0.5086 µg g^{-1} d^{-1} (highest Vmax at 30 days) and 4.24–83.42 µg (highest Vmax at 30 days), respectively.

The Vmax and Km values of CP were 0.01901 µg g^{-1} d^{-1} (at 30 days)—0.1088 µg g^{-1} d^{-1} (at 60 days) and 3.058 µg (90 days)—14.01 µg (60 days) in unamended treatments, respectively. In biochar treatments, Vmax values were 0.06712 µg g^{-1} d^{-1} (30 days)—0.01515 µg g^{-1} d^{-1} (90 days) and Km values were 3.114 µg (90 days)—103.2 µg (30 days).

The Vmax and Km values of atrazine in root were 0.1199 µg g^{-1} d^{-1} (90 days)—0.3338 µg g^{-1} d^{-1} (30 days) and 3.586–0.4252 µg in unamended soil, respectively. However, in biochar treatments, Vmax and Km values in root tissues were 0.0476 µg g^{-1} d^{-1} (90 days) − 0.3007 µg g^{-1} d^{-1} (60 days) and 1.59 µg g^{-1} (90 days) to 47.9 µg g^{-1} (60 days), respectively. Michaelis–Menten kinetics was not observed in above-ground tissues for ATZ in biochar treatments.

3.3 Presence of metabolites of chlorpyrifos and atrazine in soil and plant

In soil samples, the major metabolite of CP, i.e., 3,5,6-trichloro-2-pyridinol (TCP), was observed in C2 to C4 treatments (Additional file 1: VI). In the plant, TCP (0.025 µg g^{-1}) was observed only in the root of C4 treatment; however, it was not detected in the aboveground part of *A. paniculata*.

At 30 days, two metabolites of ATZ, i.e., desethyl atrazine (DEA) and desisopropyl atrazine (DIA) were detected in A4 and A4B treatments in soil. At 60 days, both were present in all treatments in soil. At 90 days, these atrazine metabolites were present in all treatments except A4B in soil. The concentration of both metabolites was lower in biochar treatments. In plant samples, desethyl atrazine and desisopropyl atrazine were detected in root samples of all treatments at 90 days. However, their presence in root samples at 30 and 60 days was observed in the A4 treatment. In above-ground tissues, both metabolites were detected at 60 and 90 days of sampling. No clear pattern of both metabolites was observed in above-ground tissues with the application rate of ATZ. The concentration of desmethyl atrazine and diisopropyl atrazine in plant tissues was lower in biochar treatment than without biochar treatments.

3.4 Plant growth parameters and stress enzymes

The biomass, protein, and chlorophyll content in *A. paniculata* were 55 ± 1 g, 0.22 ± 0.01 μg g^{-1} fresh weight and 30.4 ± 0.5 μg g^{-1} fresh weight in control and 73 ± 1 g, 0.22 ± 0.01 μg g^{-1} fresh weight and 32.6 ± 0.3 μg g^{-1} fresh weight in biochar treatments without pesticides, respectively. A reduction in biomass, protein, and chlorophyll contents in the plant was observed in CP and ATZ-contaminated soil in a dose–response manner compared to the control (Additional file 1: VIIa). However, a significant increase in CAT, SOD, and proline contents in plant leaves was observed under CP and ATZ stress (Additional file 1: VIIb). The biochar application significantly enhanced the biomass, protein, and chlorophyll contents as compared to only pesticide-contaminated treatments. A significant reduction in CAT, SOD, and proline in the leaves of *A. paniculata* was observed in biochar treatments. In control, the content of four metabolites, andrographolide, 14-deoxy-11,12 dihydroandrographolide, neoandrographolide, and andrograpanin of *A. paniculata* were 1.85 ± 0.01%, 0.38 ± 0.01%, 0.114 ± 0.003% and 0.011 ± 0.001% and 2.28 ± 0.03%, 0.36 ± 0.01%, 0.183 ± 0.008% and 0.009 ± 0.001% in biochar treatments without pesticides, respectively. The major secondary metabolites of *A. paniculata* i.e. andrographolide content showed a significant decrease in CP/ATZ treatments, while 14-deoxy andrographolide content in plant leaves was enhanced compared to the control (Additional file 1: VIIb). The metabolites neo-andrographolide and andrograpanin did not demonstrate any clear pattern. The biochar application enhanced the andrographolide content in the leaves of *A. paniculata* as compared to CP/ATZ alone.

3.5 Soil properties and enzymatic activities

The pH, microbial biomass, and enzymes, (alkaline phosphatase, dehydrogenase, *N*-acetyl glucosaminidase, urease, phenol oxidase, and arylsulfatase) in initial and final soil samples of control, C4, C4B, A4, and A4B treatments are reported in Additional file 1: VIII. In unamended soil, the pH of the soil in control, C4, and A4 treatments was 7.71 ± 0.12, 7.73 ± 0.10 and 7.74 ± 0.11 in the initial sample and 7.64 ± 0.11, 7.63 ± 0.11 and 7.73 ± 0.12 in the final samples, respectively. In biochar treatments, the pH of C4B and A4B soil was 8.17 ± 0.10 and 8.07 ± 0.11 in the initial sample and 8.03 ± 0.09 and 7.98 ± 0.11 in the final sample, respectively. The contents of soil microbial biomass carbon in initial and final samples were 83.7–83.9 μg g^{-1} in control, 46.8–63.7 μg g^{-1} in C4, 53.2–71.1 μg g^{-1} in C4B, 39.9–55.6 μg g^{-1} in A4, and 47.3–61.3 μg g^{-1} in A4B treatments.

The concentrations of alkaline phosphatase, dehydrogenase, *N*-acetyl glucosaminidase, phenol oxidase, arylsulfatase and urease in control soil were 112–135 μg PNP g^{-1}, 91–102 μg TPF g^{-1}; 82–96 μg PNP g^{-1}; 0.15–0.16 μg mol L-DOPA g^{-1}; 1.97–2.92 μg PNP g^{-1} and 0.25–0.27 μg NH_4-N g^{-1}, respectively. Compared to the control, a significant reduction in their concentrations (17–63%) was observed in C4 and A4 treatments. The activities of arylsulfatase, urease, *N*-acetyl glucosaminidase, and phenol oxidase were significantly increased in biochar treatments compared to unamended treatments. However, alkaline phosphatase activities were equal or lower in biochar treatments than unamended treatments. The dehydrogenase and arylsulfatase activities were enhanced in all final samples, while alkaline phosphatase, urease, and *N*-acetyl glucosaminidase displayed no clear pattern between the final and initial soil samples.

3.6 Changes in the microbial community

In 16SrRNA sequencing, total sequences of 204,282, 351,579, 227,538, 344,540, and 285,481 were obtained in initial samples of control, A4, A4B, C4, and C4B treatments, respectively. While total sequences of 827,490, 962,123, 894,682, 1,189,609, and 314,743 were obtained in final samples of control, A4, A4B, C4, and C4B treatments, respectively. Shannon and Simpson's diversity index in different treatments varied from 4.92 to 5.22 and 0.978 to 0.989 (Additional file 1: IXa). Principal Coordinate Analysis (PCoA) plots were constructed using Bray Curtis, weighted and unweighted unifrac measures for beta diversity (Additional file 1: IXa). The three factors with a percentage variation of 16.65% (PC1), 12.11% (PC2), and 11.75% (PC3) were observed. Plots showed that display relative species abundance between biochar amended and un-amended contaminated with CP was similar in initial samples and dissimilar in final samples. However, the opposite pattern was observed in atrazine-treated soils.

The KRONA plots represented variations in the abundance of total microbial diversity (Fig. 3). The Venn diagrams showed that biochar treatments had more unique OTUs (62–66%) than control (55%), CP (50%), and ATZ (55%) treatments in initial samples (Fig. 4a). However, CP and ATZ treatments (68 and 63%, respectively) had more unique OTUs from control (54–55%) and biochar treatments (60–63%) in the final samples.

Proteobacteria, Actinobacteria, Firmicutes, Planctomycetes, Acidobacteria, Chloroflexi, Gemmatimonadetes, and Bacteroidetes were the dominant phylum in all treatments. The abundance of Actinobacteria, Firmicutes, Planctomycetes, Chloroflexi, and Gemmatimonadetes was higher in CP/ATZ contaminated soil than in control in initial samples. In initial samples, a higher abundance of Proteobacteria and Bacteroidetes in biochar treatments was observed than in CP/ATZ alone treatments.

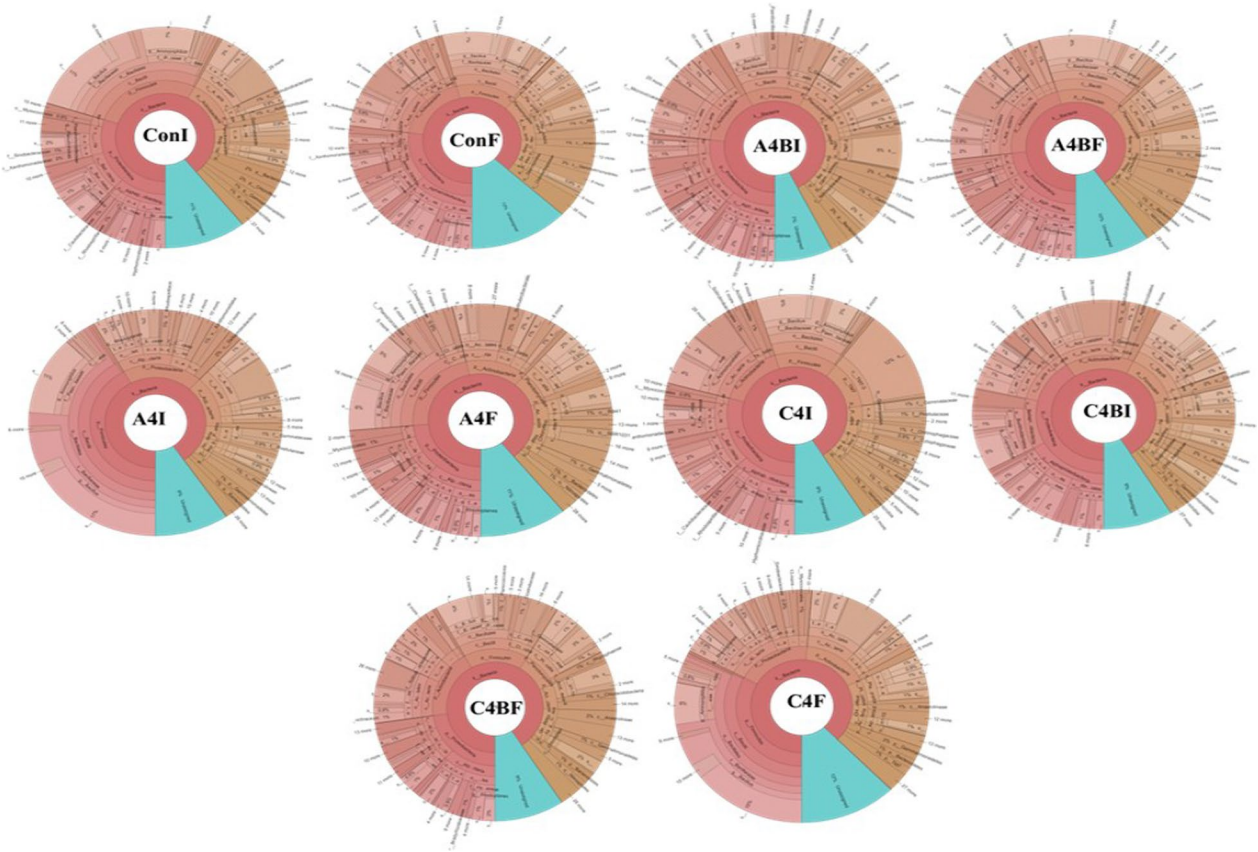

Fig. 3 KRONA plots showing the variations in the abundance of the total microbial community (from phylum to genera based on NCBI taxonomy) among the treatments

In final samples, the abundance of Proteobacteria, Actinobacteria, Firmicutes, and Bacteroidetes was higher in biochar treatments than the alone CP/ATZ treatments (Additional file 1: IXb). Heatmaps of dominant genera in all treatments demonstrated a higher abundance of genera *Flavisolibacter, Steroidobacter,* and *Alicyclobacillus* in CP treatments (Fig. 4b). In ATZ treatments, a higher abundance of the genera *Cupriavidus*, *Rhodoplanes, Planctomyces, Paenibacillus, Nitrospira,* and *Gemmata* was observed. The genera *Bacillus*, *Ammoniphilus*, *Kaistobacter*, *Balneimonas*, *Steroidobacter*, *Nitrospira, Cupriavidus, Flavisolibacter, Pseudomonas,* and *Alicyclobacillus* showed higher abundance in biochar treatments (Fig. 4b). The *flexus, ochraceum, firmus, foraminis, kestanbolensis, vinacea*, *mexicana, reuszeri, ruber, fulvum,* and *humi* were the dominant species (Fig. 4c). The *flexus* was the dominant species in the initial samples of control, C4, C4B, and final samples of control, A4, A4B, and C4B. At the same time, *ochraceum* was the dominant species in initial samples of A4 and final samples of C4. The *mexicana* was the dominant species in the initial samples of A4B treatment. The relative abundance in species richness was 10.8–13% in the initial samples and 9–13% in the final samples.

Variations in the functional order of the genome are shown in the PICRUSt analysis (Fig. 5). The functional order of metabolism, genetic information, environmental information, cellular process, and the organismal system was 51.08–51.8%, 14.8–16.01%, 13.36–16.01%, 3.7–4.1%, and 0.75–0.85%, respectively. A higher proportion of predicted genes for nucleotide, energy, carbohydrate, amino acid metabolism, and xenobiotic biodegradation and metabolism: atrazine degradation, cellular process, cell motility, membrane transport system, translation, and transcription, were observed in biochar treatments, particularly in initial samples. Gene copy numbers in the phosphotransferase system were lower in un-amended ATZ treatment as compared to its biochar amendments, while they were higher in un-amended CP-contaminated soil as compared to biochar treatments. In biochar amendments, most functional genomes were higher in CP-contaminated soil than in ATZ-contaminated soil.

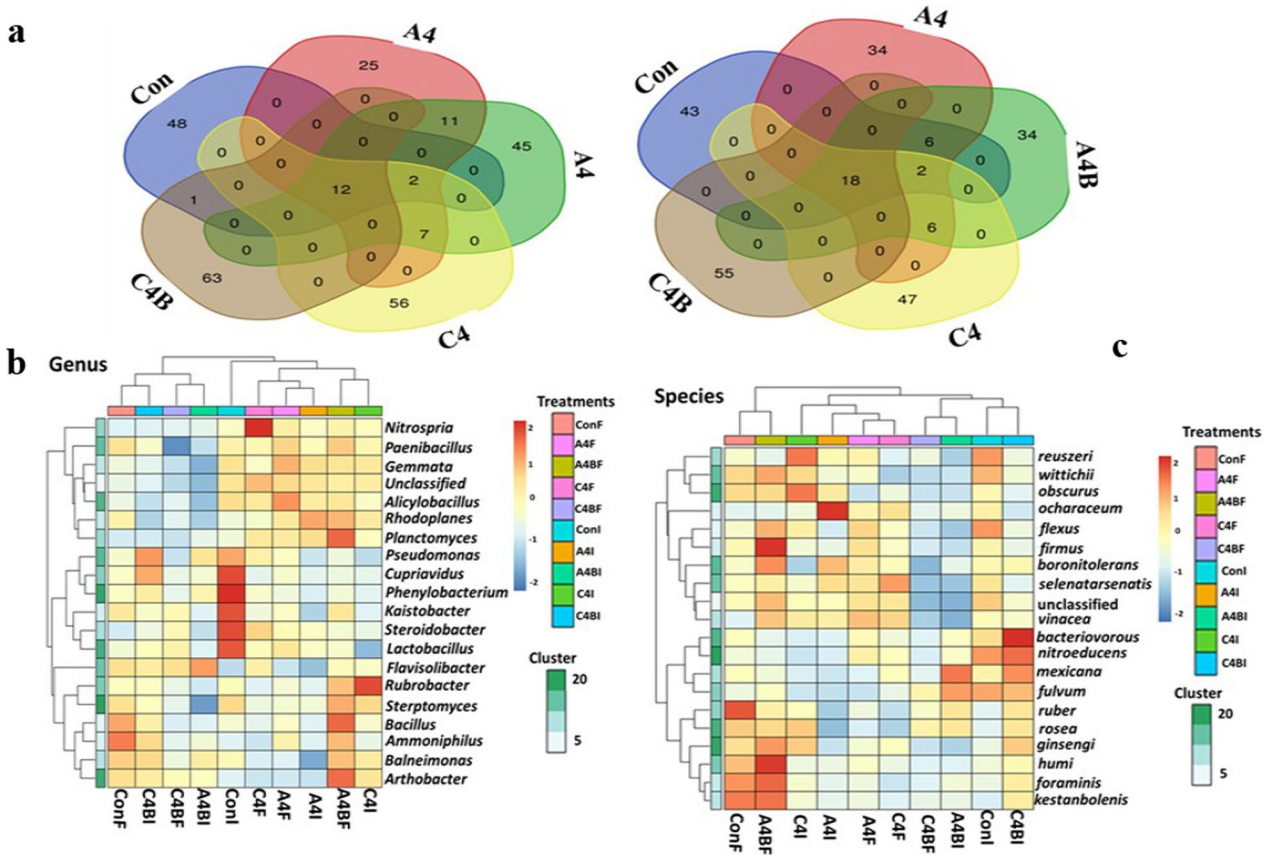

Fig. 4 **a** Venn diagrams based on the abundance of genera **b** Heatmap of dominating genera in different treatments **c** Heatmap of dominating species in different treatments [ConI and CONF: Initial and final samples of control; A4I and A4F: Initial and final samples of atrazine treatment at 8 mg kg^{-1} application rate; A4BI and A4BF: Initial and final samples of atrazine + biochar treatment at 8 mg kg^{-1} application rate; C4I and C4F: Initial and final samples of chlorpyrifos treatment at 12 mg kg^{-1} application rate; C4BI and C4BF: Initial and final samples of chlorpyrifos + biochar treatment at 12 mg kg^{-1} application rate]

3.7 Statistical analysis

The correlation analysis among the abundance of genera, functional genome, soil enzymes, pH, half-life of CP/ATZ, and plateau was performed to examine the association of major genera and soil enzymatic activities with dissipation of CP/ATZ. The half-life of CP/ATZ and plateau of SFO were negatively associated with *Balneimonas*, *Cupriavidus, Gemmata*, *Rubrobacter, Flavisolibacter*, and *Pseudomonas* (r = − 0.570 to − 0.710) (Additional file 1: Xa). The degradation rate constant was positively correlated with *Balneimonas*, *Flavisolibacter,* and *Rhodoplanes* (r = 0.53 to 0.61) (Additional file 1: Xa). CP/ATZ content in soil has a positive association with alkaline phosphatase and a negative association with *Bacillus*, *Kaistobacter*, *Pseudomonas, Steroidobacter,* dehydrogenase, and soil microbial biomass carbon Additional file 1: Xb). The functional genome cell processes, environmental information processing, genetic information processing, metabolism, and organismal systems were positively correlated with pH (r = 0.744 to 0.794), *Cupriavidus* (r = 0.753 to 0.846), *Pseudomonas* (r = − 0.835 to 0.849), *Flavisolibacter* (r = 0.484 to 0.589) (Additional file 1: Xc).

Principal component applied on CP/ATZ concentration in soil, root, and above-ground tissues, all plant parameters, BCF, and TF to examine the similarity/dissimilarity between unamended and the biochar amended treatments. PCA demonstrated a total variance of 82% (Fig. 6a) with two components, PC1 (57.65%) and PC2 (15.7%). The plot of PC1 and PC2 showed that biochar treatments were separated with alone CP/ATZ treatments (Fig. 6a). For further explanation of that data set, the correspondence analysis (CA) was performed firstly by taking plant parameters, CP/ATZ concentration in soil, root, and above-ground tissues, BCF, and TF, and secondly using soil enzymes, abundance of dominant genera, and kinetic parameters of CP/ATZ dissipation of initial and final CP/ATZ alone and with biochar treatments. In this first case (Fig. 6b), the first two dimensions weighed 66.7% and 20.7%. The

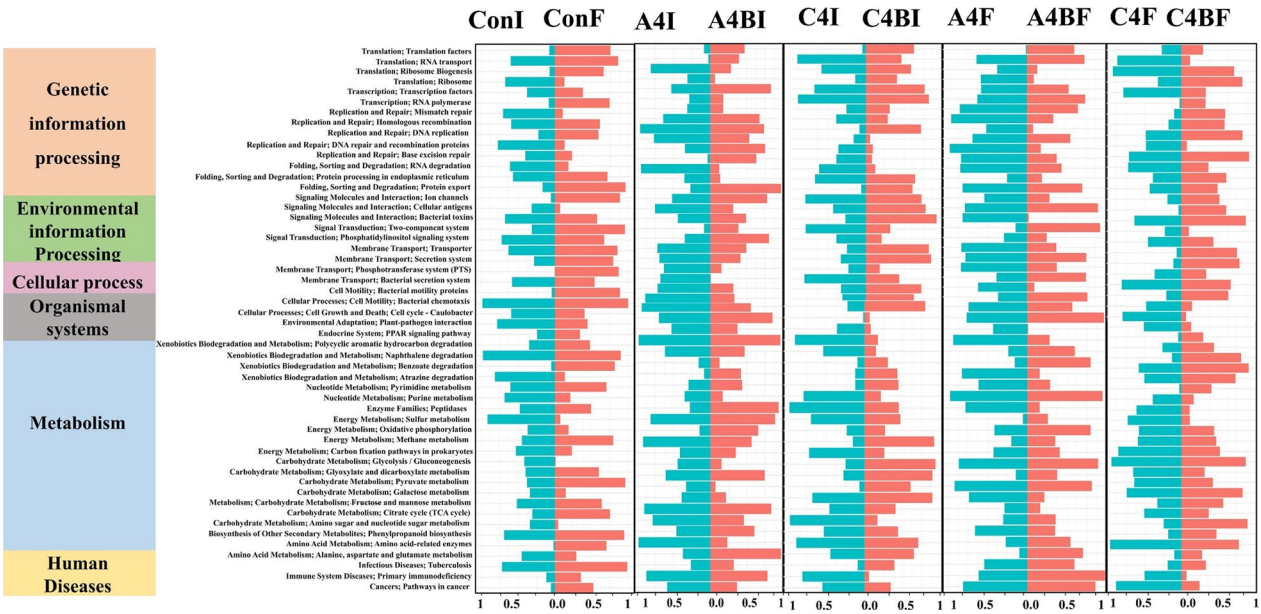

Fig. 5 PICRUSt predicted the metabolic function profiles of bacterial community in different treatments [ConI and CONF: Initial and final samples of control; A4I and A4F: Initial and final samples of atrazine treatment at 8 mg kg^{-1} application rate; A4BI and A4BF: Initial and final samples of atrazine + biochar treatment at 8 mg kg^{-1} application rate; C4I and C4F: Initial and final samples of chlorpyrifos treatment at 12 mg kg^{-1} application rate; C4BI and C4BF: Initial and final samples of chlorpyrifos + biochar treatment at 12 mg kg^{-1} application rate]

grouping of all biochar treatments was observed with biomass, protein, chlorophyll, and 14-deoxy-11,12-didehydroandrographolide (DDA) content. The treatments A4 and A4B were paired with TF and initial pesticide content in the soil. However, other pesticide treatments were grouped with CP/ATZ in soil, the root, aboveground plant tissues, and stress enzymes. In the second case (Fig. 6c), CA explained 44.56 and 37.37% of weights for the first two dimensions. The treatment A4 was paired with an abundance of *Cupriavidus, Rhodoplanes, Planctomyces, Paenibacillus, Nitrospira, Gemmata,* and soil enzyme alkaline phosphatase. However, initial samples of A4 and C4B and final samples of A4B were paired with an abundance of *Pseudomonas, Bacillus*, *Ammoniphilus, Rubrobacter*, *Balneimonas, Kaistobacter,* and soil enzymes *N*-acetyl glucosaminidase, urease, and phenol oxidase. The treatment's initial samples of C4 and final samples of C4B were associated with the rate constant (K), an abundance of *Flavisolibacter,* and soil enzyme dehydrogenase. The final sample of C4 was associated with plateau (PLT), the abundance of *Alicyclobacillus,* and *Steroidobacter* genera.

Further, the principal component was applied to soil (enzymes, dominant genera, CPT/ATZ dissipation kinetics) and plant parameters (Vmax and Km values of root and above-ground tissues of the plants) to examine the association of the parameters with each other (Fig. 6d). The four components were obtained with a variance of 83.5%. The first two factors were 32.1% and 23.4%. The PC1 and PC2 plots demonstrated that the dissipation rate constant (K) of CP/ATZ, Km, Vmax of the root, and Km of above-ground tissues were paired with an abundance of *Pseudomonas* and *Flavisolibacter*. Vmax of above-ground tissues was paired with CP/ATZ content in the soil, plateau of SFO kinetics, alkaline phosphatase activities, and abundance of *Cupriavidus.* The soil enzyme activities dehydrogenase, *N*-acetyl glucosaminidase, soil microbial biomass carbon, phenol oxidase, and urease were associated with *Balneimonas*, *Kaistobacter*, *Rubrobacter*, *Ammoniphilus*, and *Bacillus*. The D-50 was associated with *Steroidobacter Gemmata*, *Planctomyces*, *Rhodoplane*, *Paenibacillus,* and *Nitrospira*.

4 Discussions

4.1 *Effect of biochar on microbial community, enzymes, and degradation of* chlorpyrifos and atrazine *in soil*

The bio-toxicity and the microbial degradation of pesticides are controlled by factors such as soil microbial biomass, and interaction between pesticide and soil particles (Marín-Benito et al. 2021). Generally, pesticides adhere to soil particles and occupy the organic mineral surface as well as the cell surface of microbes, which hinders the interaction between active sites of enzymes and soluble substrates. Consequently, the metabolic and enzymatic

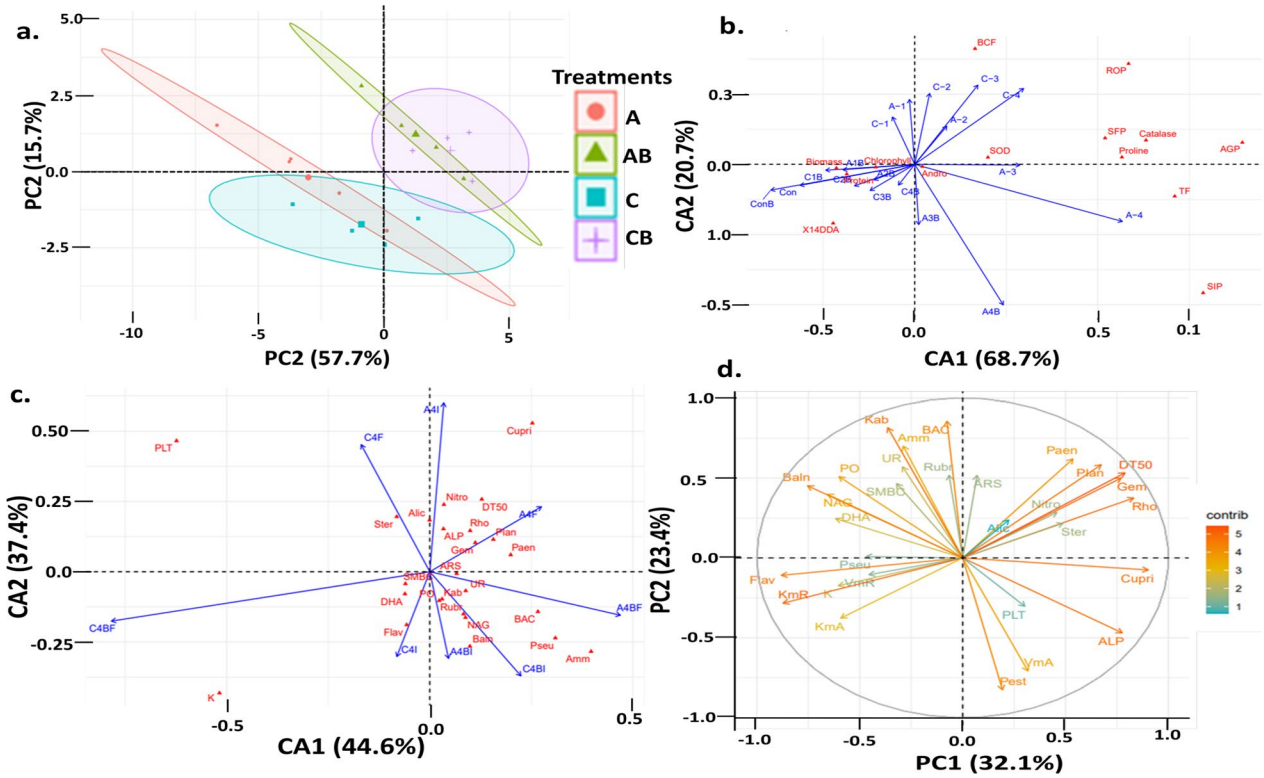

Fig. 6 **a** Principal component analysis **b** correspondence analysis of the relationship among plant variables in different treatments **c** correspondence analysis of the relationship among variables of soil in different treatments **d** principal component analysis [A: atrazine all treatments, AB: atrazine + biochar all treatments, C: chlorpyrifos all treatments, AB: chlorpyrifos + biochar all treatments, BM: Biomass, CHL: Chlorophyll, PRT: Protein; PRO: Proline, ROP and AGP: CP/ATZ in Root and aboveground tissues, CP/ATZ content in root and above ground tissues, PI and PF: CP/ATZ content in initial and final (after 90 days) soil, PLT: Plateau; DT 50: half-life of CP/ATZ in soil; K is dissipation constant of CP/ATZ in soil, alkaline phosphatase: ALP, dehydrogenase: DHA, *N*-acetyl glucosaminidase: NAG, Urease: UR, phenol oxidase: PO and aryl sulphatase: ARS; SMBC: soil microbial biomass carbon; KmR and KmAB are the Km values of CP/ATZ in root and above ground tissues, VmR and VmAB are the Vmax values of CP/ATZ in root and above ground tissues, BAC: *Bacillus*, Amm: *Ammoniphilus*, Kab: *Kaistobacter*, Rho: *Rhodoplanes*, Gem: *Gemmata*, Baln: *Balneimonas*, Ster: *Steroidobacter*, Plan: *Planctomyces*, Nitro: *Nitrospira*, Cupr: *Cupriavidus*, Rubr: *Rubrobacter*, Flav: *Flavisolibacter*, Paen: *Paenibacillus*, Pseu: *Pseudomonas*, Alic: *Alicyclobacillus*]

activities of microbes in the soil are altered (Papazlatani et al. 2019). In addition, the formation of metabolites that have higher toxicity than the parent molecule also affect adversely the mineralization of pesticides. The availability of pesticides to microbes may also have an inhibitory effect on their growth. Hence, a significant reduction in soil enzymatic activities and microbial biomass was observed in CP and ATZ contaiminated soil. However, the addition of biochar enhanced soil properties such as OC, pH, and WHC leading suitable conditions for microbial growth (Oladele 2019). In addition, biochar has good adsorbent properties which reduce their bioavailability and accessibility of toxicants to the microbes (Meng et al. 2019). Biochar also reportedly provides carbon, nutrients, habitat, and energy to microbes for their growth (Yadav et al. 2019, 2023; Tao et al. 2020). This can explain the positive effect of biochar on reducing the toxicity of CP/ATZ to soil microbial biomass carbon and soil enzymatic activities in this study. Further, the upregulation of functional genes associated with amino acids and carbohydrates in biochar treatments showed an acceleration in the growth and metabolism of bacteria. Subsequently, more dispassion of CP and ATZ in biochar treatments also reduced the toxic effect on microbes (Liang et al. 2020; Sun et al. 2023). The antagonistic relationship between SMBC and the half-life of CP/ATZ and the synergistic relationship of soil pH with major functional genome further confirmed these findings (Additional file 1: Xc). The denitrification of ATZ by anaerobic respiration and more hydrolysis of CP was reported in soil having higher microbial biomass carbon in that soil. (Singh et al. 2022b). However, the magnitude of these processes depends upon the presence of CP and ATZ degrader microbes in the soil. The upregulation of functional genomes associated with xenobiotic biodegradation and metabolism in biochar treatments indicated

an increase in the abundance of pesticide degraders (Sun et al. 2020).

The pesticides in soil altered the abundance of selected phylum due to either their toxic effects or accelerated the degrader's community by supplying substrate. The *Bacillus (*phylum Firmicutes) and *Pseudomonas* (phylum Proteobacteria) were reported tolerant and degraders for CP (Guo et al. 2020). Acinetobacter (carry atzBC and trzN genes) and *Pseudomonas* (carry atzC gene) were known for the metabolism of atrazine (Liu et al. 2023c). *Ochraceum* (carrying the thrB gene) is known for its denitrifying and phosphorylation properties (Gupta and Gupta 2021). Their higher abundance in CP and ATZ contamination suggested their involvement in CP/ATZ degradation. The positive effect of biochar on the abundance of phyla Proteobacteria, Actinobacteria, Firmicutes, and Bacteroidetes due to its porous structure, high carbon and cation exchange capacity, and presence of functional groups was reported earlier in pesticide-contaminated soils (Huang et al. 2020; Manasa et al. 2020).

The dominant genera *Flavisolibacter, Bacillus, Pseudomonas, Balneimonas*, *Kaistobacter*, *Rubrobacter*, and *Ammoniphilus* present in soil were known for their role in xenobiotic mineralization, repairing the soil and plant growth-promoting (Lin et al. 2018; Dhakar et al. 2023; Liu et al. 2023a) They higher abundance in biochar treatments may be linked with more dissipation of CP and ATZ (Fig. 6c). The association of the abundance of *Flavisolibacter* with dehydrogenase and soil microbial biomass carbon explained the mineralization of complex organic compounds in soil (Liu et al. 2020a). The genera *Rubrobacter* was reported to enhance the degradation of ATZ and reduce its toxicity to plants (Aguiar et al. 2020; Liu et al. 2020b). In our study, most of the dominant species were associated with the genera *Bacillus,* which is known for the degradation of atrazine, CP, and methyl parathion (Tang et al. 2017). *Bacillus flexus* was reported for phosphorus solubilization, degradation of pyrethroids, and polyaromatic hydrocarbons (Gousia Gani et al. 2021). Likewise, association of *Pseudomonas* with alkaline phosphatase, urease, and *N*-acetyl glucosaminidase suggested their involvement in the mineralization of C, N, and P (Asamba et al. 2022; Singh et al. 2022b). The role of *Pseudomonas sp.* in phosphate solubilization and bioremediation of persistent herbicide atrazine and its toxic metabolites was reported previously (Behera et al. 2017; Duhan et al. 2023). *Pseudomonas mexicana* novel bacteria was reported for conversion of nitrates into nitrites and plant growth promotion in contaminated agricultural soils (de los Santos Villalobos et al. 2023). The dominance of *mexicana* in A4B suggested more nitrogen fixation in biochar treatment. The genera *Kaistobacter* was identified as soil-indigenous degraders for atrazine mineralization (Lin et al. 2018).

Generally, the high adsorption capacity of biochar impeded the dissipation of pesticides in soil (Song et al. 2023). However, contrasting results in our study for biochar treatments can be explained by more abundance of genera involved in CP/ATZ degradation. The variability in dissipation rate in different treatments was associated with the concentration of CP/ATZ in soil, their availability to microbes, and the toxicity of the metabolites produced. It has been reported that higher concentrations of pesticides may act as a substrate for microbes and provide energy. This, in turn, enhances their growth, leading to a lower half-life of CP and ATZ (Singh et al. 2020). However, the accumulation of more toxic metabolites inhibited microbial growth and restricted pesticide mineralization. The production of TCP slows down bacterial activities in soil and lowers the degradation rate of CP due to its higher antibacterial activities and affinity to bind with DNA (Bhende et al. 2022). However, desethyl atrazine (DEA) and desisopropyl atrazine (DIA) have similar toxicity as parent material (Yang and Zhang 2020). Therefore, the degradation rate of ATZ was more than that of CP in the present study.

4.2 *Effect of biochar on plant growth and* chlorpyrifos and atrazine *uptake*

The phytotoxicity of CP and ATZ in plants causes the denaturing of proteins, lipids, and nucleic acids hampering normal plant growth (Tripathi et al. 2021). CP and ATZ demonstrated adverse effects on the growth, protein, and chlorophyll contents of *A. paniculata*. The toxicity of CP and ATZ exposure to plants may lead to metabolic disorders like overproduction of reactive oxygen species and cellular oxidative damage (Homayoonzadeh et al. 2021). The enhanced level of SOD, CAT, and proline under CP and ATZ exposure displayed induction of oxidative stress in *A. paniculata.* The epigenetic modification and jasmonate signaling pathway activation were reported in the presence of atrazine (ATZ) in rice crops (Ma et al. 2021). However, the restoration of these adverse oxidative stress by biochar was due to the higher dissipation of CP/ATZ in soil and restriction in the uptake of CP and ATZ in plants (You et al. 2019; Ju et al. 2020).

The hydrophobic/hydrophilic nature and mineralization of pesticides in plants controlled the accumulation of CP and ATZ in the roots and their lower upward translocation. The hydrophobic molecules easily adsorbed the lipid material of the root, hence more accumulated in the root, as observed in our study (Liu et al. 2021). Previously, more uptake of atrazine in the root was reported than shoot (Tripathi et al. 2021). The molecular weight of the

pesticides is another controlling factor for their upward translocation due to the slow diffusion rate of large-sized molecules through root cell membranes (Chuang et al. 2019). In the present study, the lower molecular weight of atrazine compared to CP could be the reason for its higher translocation in *A. paniculata*.

The uptake and translocation of organic pollutants occur either by active transport (required transporter followed single first-order kinetics) or by passive transport (adsorbed/diffusion by root hair and travel via the symplastic pathway to the xylem) and followed SFO (Wang et al. 2019). Our results demonstrated that diffusion is the dominant mechanism for CP which could be due to its hydrophobic nature and in line with previous reports (Wang et al. 2019). However, active transport was the dominant pathway for ATZ uptake as it is a weak base. Also, the mineralization of ATZ in plants may be the reason for non-fitting in first-order kinetics. The presence of DEA and DIA in plants in our study aligned with these findings.

Not fitting a single first order in biochar treatments could be due to the alteration in the diffusion of pesticides by biochar (Carter et al. 2014). For example, biochar may immobilize the CP at lower concentrations by biochar restricting its quick diffusion. However, at higher concentrations, higher catabolic activities of soil microbes in biochar caused rapid degradation of pesticides and limited quick diffusion. The changes in the soil properties by biochar may also alter enzymatic and metabolic activity within plants and affect pesticide metabolism in plants (Tao et al. 2021). The reduction of plateau and half-life of CP and ATZ in plant tissues of biochar treatments was in line with these findings.

A good fit for the Michaelis–Menten equation described the CP/ATZ uptake process as carrier-mediated (Liu et al. 2021). It may be possible that some protein present or induced by pesticide stress participates in the active transport of the CP and ATZ in the *A. Paniculata.* The active transport of hydrophobic organophosphate esters was reported in wheat by nonspecific lipid transfer proteins (nsLTPs) (Liu et al. 2022). The decrease in the Km value (increase in affinity to bind) with time suggested that the induction of the protein involved in transportation occurs with time. The reduction in affinity of CP/ATZ to bind and reaction velocity in biochar treatment suggested less induction of carrier protein. Biochar treatments in soil may also produce some inhibitors that reduce the affinity (high Km) of CP and ATZ in plants. Various inhibitors are reported in the literature, slowing down pesticide binding in plant tissues (Gressel 2020). In our study, the clustering of Vmax and Km of root and Km of aboveground plant tissues with *Flavisolibacter* and *Pseudomonas* suggested these genera may, besides their degradation potential for CP/ATZ, play an essential role in the uptake of CP and ATZ. They may also participate in degrading CP/ATZ present in plant tissues. The hydrolysing potential of endophytic bacterial strain, *Pseudomonas sp.* BF1-3 isolated from Balloon flower (*Platycodon grandiflorum*) root was reported for CP (Barman et al. 2014). Overall, biochar treatment provided habitat/growth to some degraders or accelerated the development of endophytic bacteria with CP or ATZ degradation potential. This area needs to be studied further.

5 Conclusions

The study demonstrated that the application of biochar reduced the half-life of CP and ATZ from 8.3–74.6 days to 6.6–41.1 days and 21–145 days to 40–76 days, respectively, depending upon their concentrations in soil. Applying biochar in soil improved the pH, bulk density, water-holding capacity, and microbial carbon. The use of biochar in the soil also increased the population of pesticide degrader and plant growth-promoting genera such as *Flavisolibacter, Pseudomonas, Balneimonas, Kaistobacter, Rubrobacter, Ammoniphilus*, and *Bacillus*. This increase led to the rapid degradation of CP/ATZ in the soil, reduction in pesticide toxicity to microbes and improvment in plant growth. Applying biochar also modified the uptake kinetics of pesticides in plant tissues by reducing their binding affinity in plant tissues. This study is the first to demonstrate the role of biochar in the uptake kinetics of CP/ATZ. Further studies are needed to understand the process thoroughly.

Supplementary Information

The online version contains supplementary material available at https://doi.org/10.1007/s42773-024-00306-5.

Additional File 1 contains Supplementary Ia Properties of soil; Supplementary II CP and ATZ concentration in soil, root, and above-ground tissues of A. paniculata, and their bio-concentration factors (BCF) and translocation factor (TF). Alphabets showed the significnat variation ($p = 0.001$) among the treatments; Supplementary III Parameters of simple first decay of CP and ATZ in soil with and without biochar; Supplementary IV Parameters deduced from first order kinetics with and without biochar in plant; Supplementary V Parameters of Michaelis-Menten for CP and Atrazine uptake in A. Panniculata; Supplementary VI: Metabolites of CP and ATZ in soil and plant tissue; Supplementary VIIa Variations in biomass, chlorophyll, and protein content of the plant among the treatment. Alphabets showed the significant variation ($p = 0.001$) among the treatments; Supplementary VIIb Variations in secondary metabolites, proline, catalase, and SOD of the plant among the treatment. Alphabets showed the significant variation ($p = 0.001$) among the treatments. ANDRO: andrographolide 14 DDA: 14-deoxy-11,12 dihydroandrographolide, NEO neoandrographolide and AndroG andrograpanin; Supplementary VIII Variations in soil enzymes among the treatment. Alphabets showed the significant variation ($p = 0.001$) among the treatments SMBC: soil microbial biomass carbon, ALP:

alkaline Phosphatase; ARS: aryl sulphatase; NAG: N-acetyl glucosaminidase DHA: dehydrogenase, PO: phenol oxidase; Supplementary IXa Shannon index and Simpson's diversity index (SDI) of the microbial community of soil; Supplementary IX b Heatmaps of the abundance of phylum and class of microbial community of soil in different treatments ; Supplementary Xa Correlation between kinetic parameters and abundance of major genera [BAC: Bacillus, Amm: Ammoniphilus, Kab: Kaistobacter, Rho: Rhodoplanes, Gem: Gemmata, Baln: Balneimonas, Ster: Steroidobacter, Plan: Planctomyces, Nitro: Nitrospira, Cupr: Cupriavidus, Rubr: Rubrobacter, Flav: Flavisolibacter, Paen: Paenibacillus, Pseu: Pseudomonas, Alic: Alicyclobacillus]; Supplementary Xb Correlation of the kinetic parameters, and abundance of major genera with soil enzymes; Supplementary Xc Correlation between the abundance of major genera and soil enzymes with soil microbes functional genome.

Acknowledgements
The authors are thankful to the Director, Central Institute of Medicinal and Aromatic Plant, Lucknow, UP, India. They are also thankful to the Department of Biotechnology (DBT), New Delhi **(**BT/PR24706/NER/95/822/2017) under the twinning program and CSIR-CIMAP (MLP-10) for financial assistance. CIMAP manuscript number is CIMAP/PUB/ 2023/141.

Author contributions
RPS: Investigation, formal analysis; RY: Formal analysis; VP: Formal analysis; AS: Data curation, MS: Formal analysis; KS: Methodology, funding acquisition; PK: Conceptualization, funding acquisition, writing—review and editing.

Funding
Not applicable.

Availability of data and materials
Not applicable.

Declarations

Competing interests
The authors declare that they have no known competing financial interests or personal relationships that could have appeared to influence the work reported in this paper.

Author details
[1]Crop Production and Protection Division, CSIR-Central Institute of Medicinal and Aromatic Plants, Lucknow 226015, India. [2]Phytochemistry Division, CSIR-Central Institute of Medicinal and Aromatic Plants, Lucknow 226015, India. [3]Academy of Scientific and Innovative Research (AcSIR), Ghaziabad 201002, India.

Received: 11 September 2023 Revised: 29 January 2024 Accepted: 3 February 2024
Published online: 01 March 2024

References

Acosta-Martinez V, Cano A, Johnson J (2018) Simultaneous determination of multiple soil enzyme activities for soil health-biogeochemical indices. Appl Soil Ecol 126:121–128

Aguiar LM, de Freitas SM, de Laia ML, de Oliveira MJ, da Costa MR, Gonçalves JF, Silva DV, Dos Santos JB (2020) Metagenomic analysis reveals mechanisms of atrazine biodegradation promoted by tree species. Environ Pollut 267:115636

Anbarasan R, Jaspin S, Bhavadharini B, Pare A, Pandiselvam R, Mahendran R (2022) Chlorpyrifos pesticide reduction in soybean using cold plasma and ozone treatments. Lwt 159:113193

Andrade R, Silva SHG, Weindorf DC, Chakraborty S, Faria WM, Guilherme LRG, Curi N (2020) Tropical soil order and suborder prediction combining optical and X-ray approaches. Geoderma Reg 23:e00331

Arnon DI, Whatley F (1949) Is chloride a coenzyme of photosynthesis? Science 110(2865):554–556

Asamba MN, Mugendi EN, Oshule PS, Essuman S, Chimbevo LM, Atego NA (2022) Molecular characterization of chlorpyrifos degrading bacteria isolated from contaminated dairy farm soils in Nakuru County. Kenya Heliyon 8(3):e09176

Bach CE, Warnock DD, Van Horn DJ, Weintraub MN, Sinsabaugh RL, Allison SD, German DP (2013) Measuring phenol oxidase and peroxidase activities with pyrogallol, L-DOPA, and ABTS: effect of assay conditions and soil type. Soil Biol Biochem 67:183–191

Barman DN, Haque MA, Islam SMA, Yun HD, Kim MK (2014) Cloning and expression of ophB gene encoding organophosphorus hydrolase from endophytic *Pseudomonas* sp. BF1-3 degrades organophosphorus pesticide chlorpyrifos. Ecotoxicol Environ Saf 108:135–141

Bates LS, Ra W, Teare I (1973) Rapid determination of free proline for water-stress studies. Plant Soil 39:205–207

Beauchamp C, Fridovich I (1971) Superoxide dismutase: improved assays and an assay applicable to acrylamide gels. Anal Biochem 44(1):276–287

Behera BC, Yadav H, Singh SK, Sethi BK, Mishra RR, Kumari S, Thatoi H (2017) Alkaline phosphatase activity of a phosphate solubilizing *Alcaligenes faecalis*, isolated from Mangrove soil. Biotechnol Res Innov 1(1):101–111

Bhende RS, Jhariya U, Srivastava S, Bombaywala S, Das S, Dafale NA (2022) Environmental distribution, metabolic fate, and degradation mechanism of chlorpyrifos: recent and future perspectives. Appl Biochem Biotechnol 194:2301

Bose S, Kumar PS, Vo D-VN (2021) A review on the microbial degradation of chlorpyrifos and its metabolite TCP. Chemosphere 283:131447

Bradford MM (1976) A rapid and sensitive method for the quantitation of microgram quantities of protein utilizing the principle of protein-dye binding. Anal Biochem 72(1–2):248–254

Cao Y, Wang L, Kang X, Song J, Guo H, Zhang Q (2023) Insight into atrazine removal by fallen leaf biochar prepared at different pyrolysis temperatures: batch experiments, column adsorption and DFT calculations. Environ Pollut 317:120832

Carter LJ, Harris E, Williams M, Ryan JJ, Kookana RS, Boxall AB (2014) Fate and uptake of pharmaceuticals in soil–plant systems. J Agric Food Chem 62(4):816–825

Casida L Jr, Klein DA, Santoro T (1964) Soil dehydrogenase activity. Soil Sci 98(6):371–376

Chao W-W, Lin B-F (2010) Isolation and identification of bioactive compounds in *Andrographis paniculata* (Chuanxinlian). Chinese Medicine 5:1–15

Cheng H, Xing D, Twagirayezu G, Lin S, Gu S, Tu C, Hill PW, Chadwick DR, Jones DL (2023) Effects of field-aging on the impact of biochar on herbicide fate and microbial community structure in the soil environment. Chemosphere 348:140682

Chuang W-C, Chen J-W, Huang C-H, Shyu T-H, Lin S-K (2019) FaPEx® multipesticide residues extraction kit for minimizing sample preparation time in agricultural produce. J AOAC Int 102(6):1864–1876

Das P, Khare P, Singh RP, Yadav V, Tripathi P, Kumar A, Pandey V, Gaur P, Singh A, Das R (2021) Arsenic-induced differential expression of oxidative stress and secondary metabolite content in two genotypes of *Andrographis paniculata*. J Hazard Mater 406:124302

de los Santos Villalobos S, Félix Pablos CM, Valenzuela Ruiz V, Parra Cota FI (2023) *Bacillus mexicanus* sp. nov., a biological control bacterium isolated from the common bean (*Phaseolus vulgaris* L.) crop in Sinaloa, Mexico. Int J Syst Evol Microbiol 73(11):006110

Dhakar K, Medina S, Ziadna H, Igbaria K, Achdari G, Lati R, Zarecki R, Ronen Z, Dovrat G, Eizenberg H (2023) Comparative study of bacterial community dynamics in different soils following application of the herbicide atrazine. Environ Res 220:115189

Diao Z-H, Zhang W-X, Liang J-Y, Huang S-T, Dong F-X, Yan L, Qian W, Chu W (2021) Removal of herbicide atrazine by a novel biochar based iron composite coupling with peroxymonosulfate process from soil: synergistic effect and mechanism. Chem Eng J 409:127684

Dong Y, Liu X, Wu X (2023) Adsorption of diuron in black soil amended with biochar can predict its bioavailability to crops and earthworms. J Soils Sediments 23:3006

Duhan A, Bhatti P, Pal A, Parshad J, Beniwal RK, Verma D, Yadav DB (2023) Potential role of Pseudomonas fluorescens c50 and Sphingobium yanoikuyae HAU in enhancing bioremediation of persistent herbicide

atrazine and its toxic metabolites from contaminated soil. Total Environ Res Themes. 6:100052
Eissa F, Alsherbeny S, El-Sawi S, Slaný M, Lee SS, Shaheen SM, Jamil TS (2023) Remediation of pesticides contaminated water using biowastes-derived carbon rich biochar. Chemosphere 340:139819
Eivazi F, Tabatabai M (1977) Phosphatases in soils. Soil Biol Biochem 9(3):167–172
Eivazi F, Tabatabai M (1988) Glucosidases and galactosidases in soils. Soil Biol Biochem 20(5):601–606
Fan X, Chang W, Sui X, Liu Y, Song G, Song F, Feng F (2020) Changes in rhizobacterial community mediating atrazine dissipation by arbuscular mycorrhiza. Chemosphere 256:127046
Farhan M, Ahmad M, Kanwal A, Butt ZA, Khan QF, Raza SA, Qayyum H, Wahid A (2021) Biodegradation of chlorpyrifos using isolates from contaminated agricultural soil, its kinetic studies. Sci Rep 11(1):1–14
Foong SY, Ma NL, Lam SS, Peng W, Low F, Lee BH, Alstrup AK, Sonne C (2020) A recent global review of hazardous chlorpyrifos pesticide in fruit and vegetables: prevalence, remediation and actions needed. J Hazard Mater 400:123006
Garrido S, Linares M, Campillo JA, Albentosa M (2019) Effect of microplastics on the toxicity of chlorpyrifos to the microalgae Isochrysis galbana, clone t-ISO. Ecotoxicol Environ Saf 173:103–109
Gaur I, Gaur P, Gautam P, Tiwari N, Khare P, Tripathi S, Shanker K (2021) Simplified process of candidate certified reference material development for the analysis of *Andrographis paniculata* derived therapeutics. Microchem J 165:106140
Gaur P, Khan F, Shanker K (2023) Potential lipase inhibitor from underutilized part of *Andrographis paniculata*: targeted isolation and mechanism of inhibition. Ind Crops Prod 197:116623
Gousia Gani MA, Wani PA, Malik MA, Dar ZM, Masood A, Shafi S (2021) Chlorpyrifos degradation, biocontrol potential and antioxidant defence activation under pesticide stress by rhizosphere bacteria isolated from rhizosphere of peach (*Prunus persica*) plants. Chem Ecol 37:866–881
Gressel J (2020) Perspective: present pesticide discovery paradigms promote the evolution of resistance–learn from nature and prioritize multi-target site inhibitor design. Pest Manag Sci 76(2):421–425
Guo A, Pan C, Ma J, Bao Y (2020) Linkage of antibiotic resistance genes, associated bacteria communities and metabolites in the wheat rhizosphere from chlorpyrifos-contaminated soil. Sci Total Environ 741:140457
Gupta R, Gupta N (2021) Fundamentals of bacterial physiology and metabolism. Springer, Singapore
Hasanuzzaman M, Rahman M, Islam M, Salam M, Nabi M (2018) Pesticide residues analysis in water samples of Nagarpur and Saturia Upazila, Bangladesh. Appl Water Sci 8:1–6
Homayoonzadeh M, Hosseininaveh V, Haghighi SR, Talebi K, Roessner U, Maali-Amiri R (2021) Evaluation of physiological and biochemical responses of pistachio plants (*Pistacia vera* L.) exposed to pesticides. Ecotoxicology 30(6):1084–1097
Huang H, Zhang C, Rong Q, Li C, Mao J, Liu Y, Chen J, Liu X (2020) Effect of two organic amendments on atrazine degradation and microorganisms in soil. Appl Soil Ecol 152:103564
Huang X, Yang X, Lin J, Franks AE, Cheng J, Zhu Y, Shi J, Xu J, Yuan M, Fu X (2022) Biochar alleviated the toxicity of atrazine to soybeans, as revealed by soil microbial community and the assembly process. Sci Total Environ 834:155261
Jacob MM, Ponnuchamy M, Kapoor A, Sivaraman P (2020) Bagasse based biochar for the adsorptive removal of chlorpyrifos from contaminated water. J Environ Chem Eng 8(4):103904
Jain S, Khare P, Mishra D, Shanker K, Singh P, Singh RP, Das P, Yadav R, Saikia BK, Baruah B (2020) Biochar aided aromatic grass [*Cymbopogon martini* (Roxb.) Wats.] vegetation: a sustainable method for stabilization of highly acidic mine waste. J Hazard Mater 390:121799
Ju C, Li X, He S, Shi L, Yu S, Wang F, Xu S, Cao D, Fang H, Yu Y (2020) Root uptake of imidacloprid and propiconazole is affected by root composition and soil characteristics. J Agric Food Chem 68(52):15381–15389
Kumar A, Singh N (2016) Atrazine and its metabolites degradation in mineral salts medium and soil using an enrichment culture. Environ Monit Assess 188:1–12
Kumar S, Singh B, Bajpai V (2021) *Andrographis paniculata* (Burm. f.) Nees: traditional uses, phytochemistry, pharmacological properties and quality control/quality assurance. J Ethnopharmacol 275:114054
Li Z, Fantke P (2023) Considering degradation kinetics of pesticides in plant uptake models: proof of concept for potato. Pest Manag Sci 79(3):1154–1163
Liang J, Tang S, Gong J, Zeng G, Tang W, Song B, Zhang P, Yang Z, Luo Y (2020) Responses of enzymatic activity and microbial communities to biochar/compost amendment in sulfamethoxazole polluted wetland soil. J Hazard Mater 385:121533
Lin Z, Zhen Z, Ren L, Yang J, Luo C, Zhong L, Hu H, Liang Y, Li Y, Zhang D (2018) Effects of two ecological earthworm species on atrazine degradation performance and bacterial community structure in red soil. Chemosphere 196:467–475
Liu C, Lin H, Li B, Dong Y, Yin T (2020a) Responses of microbial communities and metabolic activities in the rhizosphere during phytoremediation of Cd-contaminated soil. Ecotoxicol Environ Saf 202:110958
Liu Y, Fan X, Zhang T, He W, Song F (2020b) Effects of the long-term application of atrazine on soil enzyme activity and bacterial community structure in farmlands in China. Environ Pollut 262:114264
Liu Q, Liu Y, Dong F, Sallach JB, Wu X, Liu X, Xu J, Zheng Y, Li Y (2021) Uptake kinetics and accumulation of pesticides in wheat (*Triticum aestivum* L.): impact of chemical and plant properties. Environ Pollut 275:116637
Liu Q, Gao H, Yi X, Tian S, Liu X (2022) Root uptake pathways and cell wall accumulation mechanisms of organophosphate esters in wheat (*Triticum aestivum* L.). J Agric Food Chem 70(38):11892–11900
Liu C, Han Y, Teng C, Ma H, Tao B, Yang F (2023a) Residue dynamics of florpyrauxifen-benzyl and its effects on bacterial community structure in paddy soil of Northeast China. Ecotoxicol Environ Saf 249:114390
Liu Y, Yao L, Hu B, Li T, Tian H (2023b) Adsorption behavior and residue degradation of triazine herbicides in soil amended with rice straw biochar. Agriculture 13(7):1282
Liu Z, Han L, Zhang X, Chen S, Wang X, Fang H (2023c) Core bacteria carrying the genes associated with the degradation of atrazine in different soils. Environ Int 181:108303
Luck H (1974) Estimation of catalase activity. Methods of enzymology Academic Press, New York, p 885
Ma LY, Zhai XY, Qiao YX, Zhang AP, Zhang N, Liu J, Yang H (2021) Identification of a novel function of a component in the jasmonate signaling pathway for intensive pesticide degradation in rice and environment through an epigenetic mechanism. Environ Pollut 268:115802
Mac Loughlin TM, Peluso ML, Marino DJ (2022) Multiple pesticides occurrence, fate, and environmental risk assessment in a small horticultural stream of Argentina. Sci Total Environ 802:149893
Mahajan MR, Nangare SN, Patil PO (2023) Nanosize design of carbon dots, graphene quantum dots, and metal–organic frameworks based sensors for detection of chlorpyrifos in food and water: a review. Microchem J 193:109056
Manasa M, Katukuri NR, Nair SSD, Haojie Y, Yang Z, Bo Guo R (2020) Role of biochar and organic substrates in enhancing the functional characteristics and microbial community in a saline soil. J Environ Manage 269:110737
Marín-Benito JM, Herrero-Hernández E, Ordax JM, Sánchez-Martín MJ, Rodríguez-Cruz MS (2021) The role of two organic amendments to modify the environmental fate of S-metolachlor in agricultural soils. Environ Res 195:110871
Meng L, Sun T, Li M, Saleem M, Zhang Q, Wang C (2019) Soil-applied biochar increases microbial diversity and wheat plant performance under herbicide fomesafen stress. Ecotoxicol Environ Saf 171:75–83
Mishra S, Pang S, Zhang W, Lin Z, Bhatt P, Chen S (2021) Insights into the microbial degradation and biochemical mechanisms of carbamates. Chemosphere 279:130500
Nigam N, Yadav V, Khare P, Singh RP, Das P, Shanker K, Sharma RS (2019) Exploring the benefits of biochar over other organic amendments for reducing of metal toxicity in Withania somnifera. Biochar 1:293–307
Oladele SO (2019) Changes in physicochemical properties and quality index of an Alfisol after three years of rice husk biochar amendment in rainfed rice–Maize cropping sequence. Geoderma 353:359–371
Paidi MK, Satapute P, Haider MS, Udikeri SS, Ramachandra YL, Vo D-VN, Govarthanan M, Jogaiah S (2021) Mitigation of organophosphorus insecticides from environment: residual detoxification by bioweapon catalytic scavengers. Environ Res 200:111368
Papazlatani CV, Karas PA, Tucat G, Karpouzas DG (2019) Expanding the use of biobeds: degradation and adsorption of pesticides contained in effluents

from seed-coating, bulb disinfestation and fruit-packaging activities. J Environ Manage 248:109221
Qie H, Ren M, You C, Cui X, Tan X, Ning Y, Liu M, Hou D, Lin A, Cui J (2023) High-efficiency control of pesticide and heavy metal combined pollution in paddy soil using biochar/g-C3N4 photoresponsive soil remediation agent. Chem Eng J 452:139579
Sánchez V, López-Bellido FJ, Cañizares P, Rodríguez L (2017) Assessing the phytoremediation potential of crop and grass plants for atrazine-spiked soils. Chemosphere 185:119–126
Shekhawat K, Rathore SS, Chauhan BS (2020) Weed management in dry direct-seeded rice: a review on challenges and opportunities for sustainable rice production. Agronomy 10(9):1264
Shen D, Yu K, Hu J, Zhong J, Shen G, Ye Q, Wang W (2022) Reducing environmental risks of chlorpyrifos application in typical soils by adding appropriate exogenous organic matter: evidence from a simulated paddy field experiment. Environ Pollut 293:118513
Singh S, Kumar V, Chauhan A, Datta S, Wani AB, Singh N, Singh J (2018) Toxicity, degradation and analysis of the herbicide atrazine. Environ Chem Lett 16:211–237
Singh S, Kumar V, Gill JPK, Datta S, Singh S, Dhaka V, Kapoor D, Wani AB, Dhanjal DS, Kumar M (2020) Herbicide glyphosate: toxicity and microbial degradation. Int J Environ Res Public Health 17(20):7519
Singh P, Yadav V, Deshmukh Y, Das P, Singh RP, Bano N, Kumar M, Shukla AK, Krishna A, Khare P (2021) Decoding the link between bacterial diversity and enzymatic activities of soil from *Cymbopogon flexuosus* growing dryland. Appl Soil Ecol 168:104150
Singh M, Rano S, Roy S, Mukherjee P, Dalui S, Gupta GK, Kumar S, Mondal MK (2022a) Characterization of organophosphate pesticide sorption of potato peel biochar as low cost adsorbent for chlorpyrifos removal. Chemosphere 297:134112
Singh RP, Ahsan M, Mishra D, Pandey V, Yadav A, Khare P (2022b) Ameliorative effects of biochar on persistency, dissipation, and toxicity of atrazine in three contrasting soils. J Environ Manage 303:114146
Song B, Zhou C, Qin M, Zhao B, Sang F (2023) When biochar is involved in rhizosphere dissipation and plant absorption of pesticides: a meta-analysis. J Environ Manage 345:118518
Sun T, Miao J, Saleem M, Zhang H, Yang Y, Zhang Q (2020) Bacterial compatibility and immobilization with biochar improved tebuconazole degradation, soil microbiome composition and functioning. J Hazard Mater 398:122941
Sun T, Wang F, Xie Y, Liu X, Yu H, Lv M, Zhang Y, Xu Y (2023) Biochar remediation of PFOA contaminated soil decreased the microbial network complexity. J Environ Chem Eng 11(1):109239
Tabatabai M, Bremner J (1972) Assay of urease activity in soils. Soil Biol Biochem 4(4):479–487
Tang X, Yang Y, Huang W, McBride MB, Guo J, Tao R, Dai Y (2017) Transformation of chlorpyrifos in integrated recirculating constructed wetlands (IRCWs) as revealed by compound-specific stable isotope (CSIA) and microbial community structure analysis. Biores Technol 233:264–270
Tao Y, Han S, Zhang Q, Yang Y, Shi H, Akindolie MS, Jiao Y, Qu J, Jiang Z, Han W (2020) Application of biochar with functional microorganisms for enhanced atrazine removal and phosphorus utilization. J Clean Prod 257:120535
Tao Y, Jia C, Jing J, Zhao M, Yu P, He M, Chen L, Zhao E (2021) Uptake, translocation, and biotransformation of neonicotinoid imidaclothiz in hydroponic vegetables: implications for potential intake risks. J Agric Food Chem 69(14):4064–4073
Torres LDB, Coelho LHG (2023) Atrazine Persistence in Sediment of Aquatic Microcosms. Environ Protect Res. 56–66
Tripathi P, Yadav R, Das P, Singh A, Singh RP, Kandasamy P, Kalra A, Khare P (2021) Endophytic bacterium CIMAP-A7 mediated amelioration of atrazine induced phyto-toxicity in *Andrographis paniculata*. Environ Pollut 287:117635
Wang W, Wan Q, Li Y, Xu W, Yu X (2019) Uptake, translocation and subcellular distribution of pesticides in Chinese cabbage (*Brassica rapa* var. chinensis). Ecotoxicol Environ Saf 183:109488
Yadav R, Khare P (2023) Dissipation kinetics of chlorpyrifos and 3, 5, 6 trichloro-2-pyridinol under vegetation of different aromatic grasses: Linkage with enzyme kinetics and microbial community of soil. J Hazard Mater 448:130960
Yadav V, Jain S, Mishra P, Khare P, Shukla AK, Karak T, Singh AK (2019) Amelioration in nutrient mineralization and microbial activities of sandy loam soil by short term field aged biochar. Appl Soil Ecol 138:144–155
Yadav R, Tripathi P, Singh RP, Khare P (2023) Assessment of soil enzymatic resilience in chlorpyrifos contaminated soils by biochar aided *Pelargonium graveolens* L. plantation. Environ Sci Pollut Res 30(3):7040–7055
Yang L, Zhang Y (2020) Effects of atrazine and its two major derivatives on the photosynthetic physiology and carbon sequestration potential of a marine diatom. Ecotoxicol Environ Saf 205:111359
You X, Zheng H, Ge J, Fang S, Suo F, Kong Q, Zhao P, Zhang G, Zhang C, Li Y (2019) Effect of biochar on the enantioselective soil dissipation and lettuce uptake and translocation of the chiral pesticide metalaxyl in contaminated soil. J Agric Food Chem 67(49):13550–13557
Yuan G, Huan W, Song H, Lu D, Chen X, Wang H, Zhou J (2021) Effects of straw incorporation and potassium fertilizer on crop yields, soil organic carbon, and active carbon in the rice–wheat system. Soil Tillage Res 209:104958
Zhang Y, Zhang H, Zhang A, Héroux P, Sun Z, Liu Y (2023) Remediation of atrazine-polluted soil using dielectric barrier discharge plasma and biochar sequential batch experimental technology. Chem Eng J 458:141406
Zhou Y, Qin S, Verma S, Sar T, Sarsaiya S, Ravindran B, Liu T, Sindhu R, Patel AK, Binod P (2021) Production and beneficial impact of biochar for environmental application: a comprehensive review. Biores Technol 337:125451
Zhou N, Guo H, Liu Q, Zhang Z, Sun J, Wang H (2022) Bioaugmentation of polycyclic aromatic hydrocarbon (PAH)-contaminated soil with the nitrate-reducing bacterium PheN7 under anaerobic condition. J Hazard Mater 439:129643